APPROVED FOR RELEASE: 2007/02/09: CIA-RDP82-00850R000100050024-9

APPROVED FOR RELEASE: 2007/02/09: CIA-RDP82-00850R000100050024-9

APPROVED FOR RELEASE: 2007/02/09: CIA-RDP82-00850R000100050024-9

JPRS L/8453

11 May 1979

[redacted]

EAST

EUROPE

[redacted]

TRANSLATIONS ON EASTERN EUROPE
SCIENTIFIC AFFAIRS
(FOUO 3/79)

U. S. JOINT PUBLICATIONS RESEARCH SERVICE

[redacted]

APPROVED FOR RELEASE: 2007/02/09: CIA-RDP82-00850R000100050024-9

APPROVED FOR RELEASE: 2007/02/09: CIA-RDP82-00850R000100050024-9

NOTE

JPRS publications contain information primarily from foreign newspapers, periodicals and books, but also from news agency transmissions and broadcasts. Materials from foreign-language sources are translated; those from English-language sources are transcribed or reprinted, with the original phrasing and other characteristics retained.

Headlines, editorial reports, and material enclosed in brackets [] are supplied by JPRS. Processing indicators such as [Text] or [Excerpt] in the first line of each item, or following the last line of a brief, indicate how the original information was processed. Where no processing indicator is given, the information was summarized or extracted.

Unfamiliar names rendered phonetically or transliterated are enclosed in parentheses. Words or names preceded by a question mark and enclosed in parentheses were not clear in the original but have been supplied as appropriate in context. Other unattributed parenthetical notes within the body of an item originate with the source. Times within items are as given by source.

The contents of this publication in no way represent the policies, views or attitudes of the U.S. Government.

COPYRIGHT LAWS AND REGULATIONS GOVERNING OWNERSHIP OF MATERIALS REPRODUCED HEREIN REQUIRE THAT DISSEMINATION OF THIS PUBLICATION BE RESTRICTED FOR OFFICIAL USE ONLY.

APPROVED FOR RELEASE: 2007/02/09: CIA-RDP82-00850R000100050024-9

APPROVED FOR RELEASE: 2007/02/09: CIA-RDP82-00850R000100050024-9

JPRS L/8453

11 May 1979

TRANSLATIONS ON EASTERN EUROPE

SCIENTIFIC AFFAIRS

(FOUO 3/79)

CONTENTS PAGE

APPROVED FOR RELEASE: 2007/02/09: CIA-RDP82-00850R000100050024-9

APPROVED FOR RELEASE: 2007/02/09: CIA-RDP82-00850R000100050024-9

CZECHOSLOVAKIA

UDC 528.2:629.783

MODERN METHODS AND EXPERIMENTS IN DYNAMIC SATELLITE GEODESY

Prague GEODETICKY A KARTOGRAFICKY OBZOR in Czech No 10 and 11, 1978
pp 245-249, 275-283

[Article by Engineer Jaroslav Klokocnik, Institute of Astronomy, Czechoslovak Academy of Sciences, Ondrejov]

[No 10, pp 245-249]

[Text] 1. Purposes and Methods of Dynamic Satellite Geodesy

1.1 Introduction

Satellite geodesy is concerned with determining the shape of the earth from satellite observations. There are two main approaches to satellite geodesy: geometric and dynamic.

In the former, the satellite is merely an objective, like a geodetic point on the earth's surface or a balloon in balloon geodesy. At least two ground stations from which the satellite is visible at one time take simultaneous sightings on it. From the measured directions to the satellite, the direction between the ground stations is determined. From several measurements taken simultaneously from several stations, a triangulation network can be set up. Its proportions may be taken from traditional nonsatellite measurements. Satellite triangulation can span the oceans and thus can create a worldwide reference system.

The other method requires knowledge of the satellite's orbit, i.e. the specific paramaters which at a given moment uniquely define the position and speed of the satellite in space. Observations are used to determine a satellite's orbit and changes in it, and to seek the causes of such changes. The range of critical tasks in satellite geodesy is extensive and reaches beyond the confines of geodesy, involving for example geophysics, global geology and the theory of relativity.

The main purpose of dynamic satellite geodesy is to determine the gravitational constant, to make the determination more precise (as well as providing an

APPROVED FOR RELEASE: 2007/02/09: CIA-RDP82-00850R000100050024-9

APPROVED FOR RELEASE: 2007/02/09: CIA-RDP82-00850R000100050024-9

independent control method) and to determine the geocentric coordinates of ground observation stations in a single worldwide coordinate system. The connection between observations and these results is the satellite orbit. We may say that the more precisely the orbit is determined, the more precisely the gravitational field is determined and the greater the quality and quantity of the parameters used to describe it. But the accuracy with which the orbit is determined depends on knowledge of orbital changes, and the increasing requirements for accuracy are greatly complicating the task.

In part, the orbit too is an objective, or is used in predicting the future motion of the satellite (calculation of an ephemeris), which will be tracked for a wide variety of purposes and used in satellite maneuvers and linkups of space vehicles. Tracking of satellites, determination of orbits and their changes, and determination of the gravitational constant and station coordinates may be treated as an iterative cycle.

The "primary aims" mentioned above are closely connected with determination of fluctuations in the earth's fields and variations in rotation; here the methods of satellite geodesy are gradually replacing astronomical methods.

The main stages in the dynamic method of satellite geodesy can be classified as follows:

measurements and their reduction;

determination of satellite orbits;

calculation of the gravitational constant and other unknowns. We will discuss these individual points briefly.

1.2 Measurement

By "measurement" we mean observation of a satellite from the earth's surface or from another satellite or observation of the earth's surface or the oceans from a satellite, or specific measurements made on board the satellite and transmitted to the ground. The measurement results are primarily data which are used to determine the satellite's orbit. "Reduction" of the observations is the procedure by which the raw measurements are filtered and corrected for various perturbing factors using various methods, so as to bring them into standard form for further use.

1.21 Measurements From the Earth

In observing satellites from the earth, the following types of measurement in the optical or radio parts of the spectrum are most important:

Photography with special satellite cameras. The satellite photograph is used to determine the direction to the satellite or certain topocentric coordinates of the satellite, e.g. right ascension α and declination δ. Reduction in this case entails transformation of the measured photographic coordinates of

APPROVED FOR RELEASE: 2007/02/09: CIA-RDP82-00850R000100050024-9

APPROVED FOR RELEASE: 2007/02/09: CIA-RDP82-00850R000100050024-9

the satellite observed against the stars into celestial coordinates α and δ in the catalog epoch. We emphasize that photographic observations can be used to determine only the direction to the satellite, i.e. the direction of the topocentric vector $\vec{\rho}_0$ (Fig. 1), but not the vector's magnitude $|\vec{\rho}|$.

Tracking with laser ranging instruments. The time between the emission of a laser pulse and its return from the target is measured (the satellite must be provided with a metal reflector). The topocentric distance to the satellite $|\vec{\rho}|$, i.e. the magnitude of the vector $\vec{\rho}$ but not its direction, can be calculated from the transit time. The laser system must be calibrated by measurements with a ground-based target, and the calculated distance must be corrected for scattering of the signal by the atmosphere, for the fact that the distance is not measured from the center of the satellite but from its reflecting surface, and so on.

Measurement of the doppler shift of a signal transmitted by the satellite. This measurements gives the topocentric velocity $\dot{\rho}$. The direction and distance can be determined by radar, but generally with low accuracy. The doppler measurements must be corrected for the influence of the ionosphere and troposphere and other minor effects.

Radio measurements can determine $\dot{\rho}$ and possibly the magnitude $|\vec{\rho}|$. Radio measurements are less accurate than camera and laser measurements, and for a number of reasons are unsuited to dynamic satellite geodesy.

Interferometric measurements. Two angular values are measured with a method similar to the photographic method. Reduction entails elimination of the effect of signal scattering by the atmosphere, secondary reflections near the antenna, diffraction and equipment errors.

Today, laser and doppler measurements are the most accurate. Top performance gives errors in the tenths of meters for the topocentric vector and in the tens of meters for the satellite's position in its orbit and for the geocentric coordinates of ground stations. The interferometric method which is currently being introduced into astronomy, geodesy and geodynamics has great promise as regards accuracy.

1.22 Other Methods of Measurement

In observing one satellite from another, the variation of the relative velocity is determined, e.g. from the doppler shift of transmitted signals or interferometrically. One of the satellites collects the measurements and transmits them to the earth.

The usual "earth-to-satellite" method of measuring is inverted in satellite altimetry and laser tracking of ground-based reflectors from the satellite. A radar or laser altimeter measures the vertical distance from the satellite to the nadir. From the measured transit time, the altitude can be calculated, and from this and orbital the profile of the ocean geoid can be determined.

APPROVED FOR RELEASE: 2007/02/09: CIA-RDP82-00850R000100050024-9

APPROVED FOR RELEASE: 2007/02/09: CIA-RDP82-00850R000100050024-9

The "laser scanning" project, in which a satellite-borne laser radar (range finder) scans the earth's surface at various angles and records the laser signals reflected from ground-based reflectors, is very much a new departure. Instead of a number of expensive ground-based laser ranging instruments, a single laser on the satellite does the measuring, with only "reading stations" required on the earth.

Finally, by "onboard measurements transmitted to earth" we mean gravitational gradiometry and microaccelerometry. Most of these approaches will be discused in more detail in Part 2 of this article.

Each type of measurement requires timing commensurate with the measurement accuracy. For example, the transit time in laser measurements of topocentric distances with an accuracy of ±1 meter must generally be found with an accuracy in nanoseconds (by computer), clocked to UTC world time or some other standard within a few ten-thousandths of a second.

1.3 Satellite Orbits

1.3.1 Orbital Parameters

Now, to the notion of "satellite orbit". The motion of the satellite in a given reference coordinate system is described by equations of motion, which are second-order differential equations. Their solution gives six constants: the orbital parameters. These can be the rectangular geocentric coordinates x, y and z and their first derivatives with respect to time, i.e. the velocities $\dot{x}$, $\dot{y}$ and $\dot{z}$. More informative, and extremely widely used, are the so-called "elliptical orbital parameters" (Fig. 2 [not reproduced]). These are: the major semiaxis a of the orbital ellipse; the eccentricity e of the orbit; the right ascension of the ascending node Ω , i.e. the angular distance Ω of the ascending node γ of the orbit from the vernal equinox; the argument of the perigee ω , i.e. the distance P of the perigee from the ascending node; the inclination i of the orbit to the equator; and the time at which the satellite reaches perigee, from which the right anomaly v in Fig. 2 can be calculated.

1.3.2 Perturbation of the Orbit

If the earth were a homogeneous sphere and there were no atmosphere, sun, moon or planets, once a satellite was placed in a given orbit around the earth it would remain there indefinitely. In fact, however, the orbit is subject to various perturbations, secular (long-term) and periodic (short- and long-periodic). The causes (mechanisms) of these perturbations can be classified as gravitational, nongravitational and apparent. The effect of these perturbations is to make the orbital parameters functions of time.

Gravitational perturbations of the orbit result primarily from the deviation of the earth's shape from sphericity and the nonuniform distribution of matter within the earth. The most marked secular perturbation of the orbit is

APPROVED FOR RELEASE: 2007/02/09: CIA-RDP82-00850R000100050024-9

APPROVED FOR RELEASE: 2007/02/09: CIA-RDP82-00850R000100050024-9

the effect of the earth's polar flattening on Ω and ω. This leads to a rotation of the intersections $\overline{\Omega,U}$ and $\overline{P, P'}$ (fig. 2) amounting to 360° per month. In addition, the moon and sun produce so-called "lunisolar" perturbation of the orbit. It is well known that the attractive forces of the sun and moon produce tides in the oceans and the land, and hence elastic deformations of the earth; these in turn produce other, secondary, lunisolar--tidal--perturbations of the satellite orbit.

For close-in satellites, the primary perturbation results from atmospheric drag. Atmospheric resistance has the secular effect of decreasing the major semiaxis and eccentricity of the orbit, so that the satellite comes closer to the earth's surface; the process of orbital contraction accelerates until the satellite unavoidably enters the denser layers of the atmosphere.

The nongravitational forces include, in addition to atmospheric drag, the pressure of solar radiation, both direct and reflected from the earth. Both effects are being intensively studied. Apparent forces result from the choice of the coordinate system.

1.4 The Gravitational Potential

1.4.1 Expansion as a Series of Spherical Functions

We now introduce one possible mathematical formulation of the gravitational potential and outline the procedure of using satellite observations to determine the constants $\bar{C}_{nm}$ and $\bar{S}_{nm}$ of the gravitational field along with station coordinates.

We can write the gravitational potential V in the form of a series expansion in spherical functions:

$$V = \frac{GM}{r}\left\{1+\sum_{n=0}^{\infty}\sum_{m=0}^{n}\left(\frac{R}{r}\right)^n\left(\bar{C}_{nm}\cos m\lambda + \right.\right.$$
$$\left.\left. + \bar{S}_{nm}\sin m\lambda\right)\bar{P}_{nm}(\sin\varphi)\right\}, \qquad (1)$$

where GM is the geocentric gravitational constant,

r, φ and λ are respectively the magnitude of the geocentric vector of the satellite (Fig. 1) and its geocentric latitude and longitude,

R is the length factor (major semiaxis of the reference ellipsoid), in the same units as r,

n and m are integers designating the degree and order of the functions and coefficients given below (with $n \geq m$),

$\bar{P}_{nm} \cdot \begin{matrix}\cos\\ \sin\end{matrix} m\lambda$ are spherical (Lapalace) harmonic functions of degree n,

APPROVED FOR RELEASE: 2007/02/09: CIA-RDP82-00850R000100050024-9

APPROVED FOR RELEASE: 2007/02/09: CIA-RDP82-00850R000100050024-9

$\bar{P}_{n0}$ are zonal spherical (zonal harmonic) functions or Legendre polynomials (functions) of degree n,

$\bar{P}_{nm}$ are tesseral spherical (tesseral harmonic) functions or associated Legendre functions of degree n and order m (sometimes called sectorial functions for n = m), and

$\bar{C}_{nm}$ and $\bar{S}_{nm}$ are the usual designations of the dynamic (Stokes) constants or harmonic coefficients. In equation (1) they are dimensionless. For m = 0 they are called zonal, for $m \neq 0$ they are called tesseral and for n = m they are called sectorial constants, analogously to the functions with which they are associated.

The bar indicates that these are values which have been normalized in some manner, according to international practice. The harmonic coefficients characterize the dynamic properties of the body (which could be determined numerically if we knew the distribution of matter in the body) and its external gravitational field.

We have already mentioned the secular perturbations of the node and perigee of the orbit resulting from the polar flattening of the earth. These are, with some simplification, characterized by the magnitude of coefficients $\bar{C}_{2,0}$. A nonzero coefficient $\bar{C}_{3,0}$ indocates a tendency of the body to a "pear" shape, while nonzero individual zonal coefficients indicate an asymmetry in the northern and southern hemispheres. The tesseral and sectorial harmonics define the structure of the gravitational field as a function of the geographical latitude and longitude simultaneously. Fig. 3 gives an approximate geometric interpretation [not reproduced] of the significance of the harmonic coefficients.

1.42 Determination of the Gravitational Constant and Station Coordinates From Perturbation of the Satellite Orbit

Assume that from satellite observations we have determined instantaneous (osculating) elliptical orbital parameters. If we ignore the effect of the earth's gravitational field, we can write these parameters as polynomial functions of time t and an average t_0 for the epoch of all the observations in the form

$$E_i = E_{i0} + \Delta E_i + E_{i1}(t - t_0) + E_{i2}(t - t_0)^2 + \dots, \quad (2)$$

where i and j are indices with ranges i = 1,...,6 and j = 0, 1, 2,.... E_{ij} designates each of the orbital parameters (section 1.31) in succession; E_{i0} designates the parameters at t_0.

* The parameters may be expressed in various coordinate systems; but since their definitions and transformations are outside the scope of a general article, we state only that they are given in a system defined by the earth's equator, the pole of rotation and the vernal equinox. This is usually called the "celestial" system; it is not inertial, but is subject to precession and

APPROVED FOR RELEASE: 2007/02/09: CIA-RDP82-00850R000100050024-9

APPROVED FOR RELEASE: 2007/02/09: CIA-RDP82-00850R000100050024-9

If we also take into account the perturbation part of the potential V_{gr} in equation (1), i.e.

$$V_{gr} = V - (GM/r), \tag{3}$$

then perturbations E_{gr} resulting from this perturbation potential will be added to the right side of equation (2). In the interval $t - t_0$, we have

$$E_{gr} = \int_{t_0}^{t} \dot{E}\, dt. \tag{4}$$

We seek an analytical expression for the perturbation $\dot{E}$. This requires use of the Lagrange planetary equations, which express the relationship between the perturbation potential and changes in orbital parameters. From (3) and (4),

$$\frac{dE_i}{dt} \equiv \dot{E}_i = \mathrm{L}^i(a, e, I).V_{gr}, \tag{5}$$

where E_i is again the i-th element and L^i is a linear differential operator. The reader will find specific equations in the literature cited.

Equation (5) provides a method of calculating the perturbation $\dot{E}_i$ resulting from the set of harmonic coefficients $\bar{C}_{nm}$ and $\bar{S}_{nm}$ included in the perturbation potential (3) and defined by expansion (1). In addition, for the parameters in (2) we may now write symbolically

$$E_i = E_i(E_{i0}, E_{i1}, E_{i2}, \ldots \bar{C}_{nm}, S_{nm})\ j = 1, 2, \ldots; \quad i = 1 \div 6. \tag{6}$$

Since the relation between the rectangular Cartesian coordinates x_s, y_s and z_s of the satellite in the celestial system and the elliptical orbital parameters is

$$\begin{pmatrix} x_s \\ y_s \\ z_s \end{pmatrix} = r \begin{pmatrix} \cos(v+\omega)\cos\Omega - \sin(v+\omega)\sin\Omega\cos I \\ \cos(v+\omega)\sin\Omega + \sin(v+\omega)\cos\Omega\cos I \\ \sin(v+\omega)\sin I \end{pmatrix} \tag{7}$$

$$r = a(1-e^2)/(1+e\cos v),$$

we may write the relationships between the satellite coordinates and the harmonic coefficients $\bar{C}_{nm}$ and $\bar{S}_{nm}$ symbolically as follows:

$$x_s = x_s(E_{i0}, E_{i1}, E_{i2}, \ldots \bar{C}_{nm}, \bar{S}_{nm}) \tag{8}$$

and similarly for y_s and z_s.

---

nutation. Accordingly in equation (2) there arise apparent orbital perturbations symbolized by the term ΔE_i. The coordinates of the ground-based observation stations (almost exclusively given in a system connected with the rotating earth, which is clearly the most natural) must be converted into the celestial system (movement of the pole, celestial time of observation). These measurements are generally given in a different coordinate system, e.g. right ascension and declination α, δ in the star catalog epoch. Here too we need a transformation, at least for precession and nutation from the catalog epoch to time t_0.

APPROVED FOR RELEASE: 2007/02/09: CIA-RDP82-00850R000100050024-9

APPROVED FOR RELEASE: 2007/02/09: CIA-RDP82-00850R000100050024-9

Now we should have to write equations to transform the measurements (from various satellite observations) and the geocentric coordinates X, Y, Z of the observation stations into the coordinate system in which the position of the satellite x_s, y_s, z_s is expressed (i.e. into the celestial system). After linearizing these relationships we would obtain correction equations for adjustment by least squares. Here we cannot give a detailed analysis because we do not know the definitions and transformations of the coordinate systems. We simply write

$$\bar{v} = -\bar{l} + \sum_{i=0}^{i_{max}} k_i \delta E_i + \sum_{n=2}^{n_{max}} \sum_{m=0}^{n} (k^c_{nm} \bar{C}_{nm} + k^s_{nm} \bar{S}_{nm}) + k_x \Delta X + k_y \Delta Y + k_z \Delta Z, \quad (9)$$

where $\bar{l}$ is an absolute term,

δE_i are corrections to parameters E_i in series (2), $i = 1, \ldots, 6$, $j = 0, 1, 2, \ldots, j_{max}$, k_i, k^C_{nm}, k^S_{nm}, k_X, k_Y and k_Z are symbolic representations of the coefficients of the unknowns and

$\bar{C}_{nm}$, $\bar{S}_{nm}$, ΔX, ΔY and ΔZ (together with δE_i) are the unknowns sought in the least-squares adjustment, i.e. the harmonic coefficients and corrections to the geographic coordinates X, Y and Z of the observation stations.

Equation (9) shows that it is correct to determine the gravitational constants and station coordinates simultaneously. In practice this is not always possible owing to the considerable correlation between the tesseral harmonic coefficients and the station coordinates. Accordingly, the adjustment is divided up; the satellite orbital parameters and a limited set of geopotential coefficients can be determined for approximate coordinates, after which the coordinates of selected stations are made more precise and the harmonic coefficients again refined. These "iteration cycles" are repeated using additional observational data so as to refine all the unknowns and to expand the set of harmonic coefficients and designated stations.

The upper limit n_{max} of the degree of the harmonic coefficients in equation (9) is determined experimentally with reference to the quantity and quality of the initial data. With present-day satellite measurements (cameras, lasers, doppler apparatus), the set of harmonic coefficients can be determined only up to $n_{max} = m = 10$ or 12, or higher in some cases (with orbital resonance: see Part 2). The finer structure of the gravitational field cannot be recorded from satellite orbits determined with an accuracy on the order of tens of meters by today's methods. To determine the coefficients of higher levels and orders, gravitational measurements on the land and the ocean are being taken for adjustment purposes, but this problem too is not completely solved. The most up-to-date solution of equation (1), obtained by combining satellite and gravitational methods, extends to approximately $n = m = 30$. This determines the shape of the geoid surface with an accuracy on the order of 1 meter and the geocentric station coordinates to approximately ± 10 meters.

APPROVED FOR RELEASE: 2007/02/09: CIA-RDP82-00850R000100050024-9

APPROVED FOR RELEASE: 2007/02/09: CIA-RDP82-00850R000100050024-9

1.5 Conclusion

We have given a brief and partial discussion of the purposes and "standard" methods of dynamic satellite geodesy in finding the parameters of the earth's gravitational field and other unknowns. In Part 2, we will examine satellite altimetry, gradientometry, satellite-to-satellite tracking, subsatellite projects and other modern methods impinging upon dynamic satellite geodesy with the common goal of gradually refining descriptions of the earth's gravitational field, aiming at an accuracy on the order of centimeters in determining geocentric coordinates. This accuracy will make it possible, for example, to follow movements of the earth's crust and to predict earthquakes in danger areas, to refine geophysical models of the internal structure of the earth, to conduct various oceanographic studies, to study the earth-moon tidal system in detail, to test the theory of relativity and so on.

BIBLIOGRAPHY FOR PART 1

V. Abalakin; and G. Balmino. La Geodynamique Spatiale. Notes de Cours [Course Notes on Spatial Geodesy], Lannion, 1974. CNES publication, 1976.

K. Arnold. VEFOFF. ZIPE, 7, 1972.

D. Brouwer; and G. M. Clemence. Methods of Celestial Mechanics. New York, Academic Press, 1961.

M. Mursha. Osnovy kosmicheskoy geodezii [Introduction to Space Geodesy]. II. Moscow, 1975 [in Russian].

E. M. Gaposchkin. SAO SPEC. REP. 353, 1973.

W. M. Kaula. Theory of Satellite Geodesy. Waltham, Mass., Blaisdell, 1966.

D. G. King-Hele. "The Bakerian Lecture, 1974: A View of Earth and Air," PROC. ROY. SOC. A., 178, ;975. pp 67-109.

C. A. Lundquist; and G. Veis. SAO SPEC. REP. 200, Vol. 1. 1966.

G. Veis. SAO CONTRIB. ASTROPHYS. 3, No 9 (dissertation, Ohio State Univ.), Washington, D. C., 1960.

H. G. Walter; and M. Wales. "The Differential Correction of Close Earth Satellite Orbits," Part 1, Sci. Rep. ESRO SR-7, ESD AC, 1967.

APPROVED FOR RELEASE: 2007/02/09: CIA-RDP82-00850R000100050024-9

APPROVED FOR RELEASE: 2007/02/09: CIA-RDP82-00850R000100050024-9

[No 11, pp 275-283]

[Text] 2. Modern Methods and Experiments

2.1 Introduction

In Part 1 we saw that the main purpose of dynamic satellite geodesy is to determine the earth's gravitational constant and the geocentric coordinates of observation stations. We know the main points of the approach to determination of these quantities. Now we will acquaint ourselves with results achieved to date, after which we will turn our attention to the modern methods and experiments themselves.

2.2 Models of the Earth's Gravitational Field

The set of harmonic coefficients and station coordinates forms the so-called "gravitational field model"; frequently an overall or global solution for the geopotential is discussed; among methods of satellite geodesy we will discuss a "geometric" or "dynamic" solution on the basis of the data, or a "satellite," "gravimetric (terrestrial)" or "combined" solution (where satellite measurements are combined with gravitational anomaly and other data.

The most important solutions thus far obtained are as follows:

Standard Earth I (1966), II (1969), III (1973) and V (1976) [14, 16, 17, 35];

the Goddard Space Flight Center Models of the Earth, 1-10 (1962-1977), e.g [33, 50];

GRIM 1 and 2 (1975), 1976) [5, 6], and the Dimitrijevich [13] and Rapp (e.g. [39]) gravimetric models.

The first-mentioned solution, Standard Earth I [35], is the work of the Smithsonian Astrophysical Institute (Cambridge, USA). Photographic observations from a network of 16 Baker-Nunn cameras were used to determine the complete harmonic coefficients to $n = m = 8$ (and zonal to $n = 12$) and some other coefficients. The accuracy of determination of the geocentric coordinates was about ±20 meters. One of the most up-to-date geopotential solutions, SE V [16], uses laser measurements and open-air magnetic anomaly measurements ($1 \times 1°$) from 86% of the entire earth's surface, and is complete to $n = m = 24$ (plus several "resonance terms" to $n = 37$); in addition, more than 100 station locations have been determined with an accuracy of ±3-5 meters, and a geoid surface to within ±1 meter.

Another solution is being derived by the Goddard Space Flight Center. One of the newest, combined, solutions, GEM 8 [50], contains the complete harmonic coefficients to $n = m = 25$ and the coordinates of 369 stations. Some 154,000 photographic, 76,000 laser and 332,000 radar and doppler measurements were used. The French-German GRIM 2 [6] model is a combined solution from photographic and laser measurements, results from orbital resonances for at

APPROVED FOR RELEASE: 2007/02/09: CIA-RDP82-00850R000100050024-9

APPROVED FOR RELEASE: 2007/02/09: CIA-RDP82-00850R000100050024-9

least m = 13-15, and 34,000 1 x 1° gravitational anomalies. The tesseral terms are worked out to (30, 30), and the accuracy of the geocentric coordinates is ±5-10 meters, while that of the geoid is ±3 meters.

Using the set of harmonic coefficients $\bar{C}_{nm}$ and $\bar{S}_{nm}$ from the individual solutions, it is easy to depict the "shape" of the earth by mapping the constant potential surfaces defined by equation (1) on a specific, simple mathem tically defined surface. Fig. 4 [not reproduced] shows a contour map of the shape of the geoid with respect to the rotational ellipsoid which most closely approximates the earth. The example is taken from reference [47] and represents a combination of the GEM 6 [33] combined solution with 1 x 1° gravitational anomalies.

The harmonic coefficients of higher degrees and orders have not yet been determined with sufficient reliability and accuracy [5, 6, 19, 20, 25] to make possible a determination of the shape of the geoid and the coordinates of observation stations with the centimeter accuracy which is required for various applications (see conclusion of Part 1). A number of the coefficients are strongly correlated with each other [19]. The greatest correlations are between the tesseral coefficients and station coordinates. Accordingly various alternative methods for independent control determinations and methods capable of determining the harmonic coefficients of higher degrees and orders are being sought. Below we will discuss satellite altimetry (2.3), resonant-orbit satellites (2.4), geodynamic satellites and "drag-free" systems (2.5), laser "scanning" from satellites in orbit (2.6), satellite-to-satellite tracking (2.7), gravitational gradientometry (2.8) and radiointerferometry (2.9).

2.3 Satellite Altimetry

The principle of this method is simple (see Part 1). An altimeter, i.e. a vertically-oriented radar or laser ranging instrument, is installed on board the satellite. Let us assume that measurements are being made over the ocean. Its depth is a result of the effect of tides, wind, waves and other minor influences on the geoid surface.* Accordingly, the shape of the ocean part of the geoid can be determined from altimetric measurements if the satellite orbit is known [2, 11, 36, 38, 52]. The measurement process consists of sending a signal to the surface and determining the height of the satellite above the measured location from the transit time (Fig. 5 [not reproduced]). The altitude is clearly insufficient to determine the shape of the geoid; it is necessary at the same time to track the orbit, i.e. to determine the orbital parameters (using ground-based laser ranging instruments or doppler units, for example) and to determine the instantaneous geocentric vector of the satellite.** [footnote on following page]

* Our statement about the difference between the geoid and the depth of the ocean differs from the textbook concept of the geoid. But is is required for the sake of greater accuracy. These deviations are properly the subject of geodynamic and oceanographic studies.

APPROVED FOR RELEASE: 2007/02/09: CIA-RDP82-00850R000100050024-9

APPROVED FOR RELEASE: 2007/02/09: CIA-RDP82-00850R000100050024-9

The accuracy of measurement depends primarily on the accuracy of the altimeter. Gravitational stabilization of the satellite is required in order to guarantee vertical orientation. The effect of inaccuracies in determination of the orbit can be partly compensated by a suitable computer method [7, 11].

Examples are given in Fig. 6 [not reproduced]. Here the shape of a section of the geoid surface in the Caribbean Sea based on altimetric measurements from Skylab is compared with the GEM 6 model [33, 52]. This is a typical example, and the following conclusion may be drawn: beyond systematic differences between altimetry and overall solutions (mostly less than ±20 meters) and between individual solutions, identical trends in the shape of the geoid are apparent; the overall solution for the geoid surface is smoother, while altimetry gives more detail, e.g. undersea trenches, ridges, rifts and so on.

The accuracy of the Skylab altimetric measurements was about ±1 meter, and the error in orbit determination 5 meters. The altimeter of GEOS 3 gave results accurate to within ±0.6 meters (and after filtering to within 0.2 meters); the orbit was tracked by a network of doppler stations (constantly 20-40 stations worldwide), and was determined with about a 3-meter radial error.

In addition to Skylab measurements [52], a number of authors [1], 37. 38] have used a number of GEOS 3 overflights with multiple measurements on the locations to create ocean geoids for areas of Australia and North America.

Preparations are being made to launch the oceanographic satellites SEASAT-A (May 1978) and SEASAT-B (1980) with laser reflectors on board so as to determine the ocean geoid with an accuracy of ±10 cm and to conduct oceanographic research. The orbit is to be determined by ground-based lasers and doppler instruments and by tracking from other satellites (see below).

2.4 Orbital Resonance

Orbital resonance of satellites has already been used successfully for seven years as an independent control determination of selected harmonic coefficients, and at the same time for determination of high-level and high-order coefficients whose values in comprehensive solutions are unreliable or even incorrect.

** [from preceding page] The current conception of satellite altimetry is about 14 years old [32, 34]. The first attempts to reflect a satellite signal from the surface of the earth were carried out with the Canadian ionospheric satellite 1962$\beta\alpha$ [34]. For communication purposes, a laser transmitter was used in the flight of Gemini 7 [34]; radar altimetry was used in the Apollo program; the first geodesic experiment was made from the manned Skylab station (1973) [52] (see Fig. 6 [not reproduced]); and today the results from GEOS 3 [2, 11, 38] have been made public by the US NASA organization as part of the American program on Earth and Ocean Dynamics.

APPROVED FOR RELEASE: 2007/02/09: CIA-RDP82-00850R000100050024-9

APPROVED FOR RELEASE: 2007/02/09: CIA-RDP82-00850R000100050024-9

Satellite resonance is the situation in which a satellite makes an integral number β of orbits in an integral number α of siderial days. For clarity, let us assume a satellite in a polar orbit making 15 orbits a day, so that $\beta / \alpha = 15/1$. The geographical longitude of the intersection of the orbital plane with the earth's equator will change by 24° with each pass, so that after 15 orbits the satellite will be back over the same points on the earth. This process will be repeated until perturbing forces (the effect of $C_{2,0}$, atmospheric drag and so on) change the orbit. Since this resonance condition continues for a relatively long time, repeated flight over the same parts of the gravitational field leads to a long-periodic perturbation of the orbit instead of progressive short-periodic perturbations: i.e. in the tesseral terms with m = 15 in equation (1). Perturbations in the other tesseral harmonic coefficients average out over time, but long-periodic perturbations increase and take on the character of secular perturbations, accumulating so that by using a method analogous to the ordinary method for determining the gravitational constant (Part 1) a linear combination of harmonic coefficients of order $m = \beta\gamma$ ($\gamma = 1, 2, \ldots$) is determined. These coefficients are determined separately from the others, without large mutual correlations, and more realistically than in comprehensive geopotential solutions, particularly for high values of n and m. Herein, accordingly, lie the clear advantages and disadvantages of the method. The independent determination and the high orders are advantages. A disadvantage is the small set of constants determined; moreover it is necessary to wait until resonant orbit is reached. The unquestioned advantage of the method is the fact that no particular adjusting apparatus is required either on the ground or on the satellite (quite the opposite of all other methods).

In the last few years, the orbits of about 30 satellites have been analyzed, particularly in resonance periods of 13/1, 14/1, 15/1, 29/2 and 31/2. Most of this work has been foreign: see references 18, 19, 20, 40, 41, 48, 49, 51; other studies have come from Czechoslovakia: see references 21, 22, 23, 24, 25, 44, among others.

2.5 Geodynamic Satellites and "Drag-Free" Systems

2.51 Introduction

Part 1 provided a notion of orbital perturbations, and we saw that the calculation of harmonic coefficients and coordinates of points on the earth's surface depends to a considerable extent on the accuracy of their determination. Gravitational perturbations are well known up to the rather small effects of high-order and high-degree terms (other than resonance), and the error in the orbit from incomplete knowledge of these is today on the order of tens of meters for the geocentric position of the satellite. Nongravitational perturbations such as the effect of the atmosphere and the pressure of solar radiation have been less well modeled, and the errors in the orbit may be greater. For a satellite close to the earth (less than 400 km), the atmospheric effect is dominant, but even for a high-altitude satellite not all nongravitational perturbations are eliminated: above 1,000 km, radiation pressure prevails over atmospheric drag. For geodetic and geodynamic purposes,

APPROVED FOR RELEASE: 2007/02/09: CIA-RDP82-00850R000100050024-9

APPROVED FOR RELEASE: 2007/02/09: CIA-RDP82-00850R000100050024-9

we accordingly strive to minimize the effect of nongravitational perturbations through the design of the satellite; we can do this today by two methods, either by using compact geodynamic satellites with metal reflectors or by employing so-called "drag-free" systems installed on board.

2.52 Geodynamic Satellites

The perturbing effect of the atmosphere can be expressed in the form [29]:

$$F_a = \frac{1}{2} C \rho \frac{A}{m} v^2, \qquad (11)$$

where C is the "aerodynamic" coefficient of resistance (~ 2), ρ is the air density, v is the velocity of the satellite in the resisting medium, and m/A is the transverse load, i.e. the ratio of the mass of the satellite m to the surface area A subject to atmospheric effects.

For solar radiation pressure we have [29]:

$$F_{sp} = p_k \frac{A}{m}, \qquad (12)$$

where p_k is the reflectivity (albedo).

We can see from (11) and (12) there is a direct proportionality between the size of the perturbing forces and the ratio A/m. Thus, if we wish to minimize nongravitational perturbations, we will choose small A and large m, i.e a small dense satellite. In addition, a spherical shape will be used so as to keep A/m constant.

Geodynamic satellites include the French STARLETTE, the American LAGEOS, and to some degree GEOS 3, INTERKOSMOS 17 and the SEASAT satellite which is in preparation. The first two are entirely typical: small heavy spheres with metal reflectors for passive (laser) measurement; the purpose of the experiment is to determine the geocentric coordinates of ground stations within ±5-10 cm and to monitor movements of the earth's crust.

STARLETTE [42] has been aloft since February 1975 in an orbit with a perigee of approximately 800 km and an apogee of 1,100 km. It is a sphere with a diameter of only 24 cm containing a core of U-238 (nonradioactive uranium) and an aluminum-magnesium shell with 20 triangular segments carrying a total of 60 reflectors. The total weight of the satellite is 47.3 kg, and A/m is approximately 10^{-3} m^2/kg.

LAGEOS (Laser Geodynamic Satellite) was launched in the first half of 1976 in a roughly circular orbit at an altitide of almost 6,000 km. LAGEOS is a 60-centimeter sphere with a core of brass, to which is fastened an outer layer of aluminum alloy; the satellite carries a total of 426 circular metal reflectors.

APPROVED FOR RELEASE: 2007/02/09: CIA-RDP82-00850R000100050024-9

APPROVED FOR RELEASE: 2007/02/09: CIA-RDP82-00850R000100050024-9

2.53 "Drag-Free" Systems

We have mentioned "drag-free" systems as another way of eliminating nongravitational orbital perturbations. This really involves a satellite within a satellite. The approach described below, which originated with Lange in 1964 [4, 31], was realized in the TRIAD 1 and 2 satellites [21] and is being readied in a more accurate version for the SOREL satellite; with certain modifications (CACTUS microaccelerometer) it has been used in the French D-5-B satellite [30].

We place a small, heavy sphere inside a larger, hollow sphere. Let us imagine this system in orbit: gravitational and nongravitational perturbations affect the object as a whole, but the inner sphere moves only under the influence of gravitational forces, while the nongravitational ones are eliminated. It is clear that the initial central position of the inner sphere will quickly be disturbed, and after a certain time the sphere will strike the wall of the container. There are two possibilities: to allow the collision to occur, and before that time to measure the size of the nongravitational disturbance, then to restore the interior sphere to its central position and continue cyclic measurement (the principle of microaccelerometer measurement of nongravitational forces), or to prevent shifts within the hollow sphere with as much accuracy as possible, i.e. to turn on the proper correction motor on the satellite for a moment. In this case the entire satellite will follow an orbit as if it were only under the influence of gravitational forces (drag-free system).

The satellite TRIAD 1 (US Navy), launched in September 1972, contained the DISCOS compensation system, which successfully eliminated nongravitational acceleration with an accuracy of 10^{-10} grams for a period of five months. The basis of the system was a gold-platinum ball, 2.2 cm in diameter, placed inside a larger spherical cavity (4 cm). The position of the sphere was measured in all directions, and each shift greater than 0.9 mm was compensated by rocket motors.

It is realistic to expect an accuracy of at least 10^{-13} grams in the future, which will make it possible to measure orbital effects predicted by the general theory of relativity (e.g. movement of the orbital node) and thus to test it [46].

2.6 The Laser Ranging System on a Satellite

An entirely new concept of laser measurement is the approach to detection of movements of the earth's crust proposed by Kumar and Mueller in the USA [28], as mentioned in Part 1. Instead of a number of costly laser ranging systems on the ground and satellites with metal reflectors, it was proposed to use a space-borne laser ranging system so as to measure the slant distance to various targets on the ground, the reading stations. Among various possible procedures, the authors of reference 28 propose an approach in which the laser conducts its measurements in a rapid scan over a series of ground targets: a sort of "scanning from space". The mathematical processing of measurements is the purely geometric method of satellite geodesy. Studies

APPROVED FOR RELEASE: 2007/02/09: CIA-RDP82-00850R000100050024-9

APPROVED FOR RELEASE: 2007/02/09: CIA-RDP82-00850R000100050024-9

conducted in the area of the San Andreas fault in California showed that measurements of the relative positions of ground targets using today's technology could be made with an accuracy within 5 cm in the vertical and horizontal directions. With this degree of accuracy and with an assumed movement of 4 cm per year for the Pacific and North American Plates, crustal shifts can be detected after five months' measurement, thus providing a source of warning before powerful earthquakes.

2.7 Satellite-to-Satellite Tracking

Another new method which is useful in dynamic satellite geodesy is satellite-to-satellite tracking (henceforth SST). We will outline the principle and advantages of SST. Proposals for its use to study the earth's gravitational field have been in existence for almost 10 years (e.g. reference 10), and in 1973 they found an implementation which promised practical results (see below).

The satellite measures relative velocity by doppler device or interferometer; the results are accumulated on one of the satellites, which transmits them to the ground on command (Fig. 7 [not reproduced]). Imagine two satellites in low orbit (e.g. 250-500 km above the earth), a few dozen to 200 km apart. It turns out that in such a system, the primary role in changing relative velocity is played by short-period gravitational perturbations, which can be ascribed to different effects of tesseral harmonic coefficients of high orders and degrees in various locations.

It is apparent that even here it is impossible to proceed without determining the orbit of at least one of the satellites by ground-based observation, even if the accuracy requirements are not very great [43], but this can be circumvented by having one of the satellites in a high orbit, where the orbital perturbations from tesseral harmonics and the atmosphere are small.

The unquestioned advantage of satellite-to-satellite tracking compared with ordinary measurement from the ground is the absolute independence of weather conditions, the possibility of tracking long segments of the orbit, and the organizational simplicity of the observational "campaign". When one satellite is placed in a high (generally stationary) orbit, it constitutes a "reference point," whose position may be determined with higher accuracy than the lower orbit.

A few experiments in SST have already been conducted. The Apollo space craft was tracked by doppler methods during the Soyuz-Apollo program [3] from the stationary ATS-6 satellite (1974). After conclusion of the joint flight of the orbital stations, both Apollo modules tracked each other. Gravitational anomalies were detected in Central Africa, the Indian Ocean, the Himalayas and elsewhere. Preliminary results [3] indicate that the method can be used to refine our knowledge of the earth's gravitational field. The TAS-6 also tracked the satellites GEOS 3 and Nimbus 6. The SEASATs will be equipped for the SST method; determination of the relative speed with an accuracy to within ±0.03 mm/sec and of position to within ±0.3 meters is expected.

APPROVED FOR RELEASE: 2007/02/09: CIA-RDP82-00850R000100050024-9

APPROVED FOR RELEASE: 2007/02/09: CIA-RDP82-00850R000100050024-9

An interesting application of the method with low-altitude satellites is the possible tracking of a subsatellite launched from the planned Spacelab [43]. To measure the radial velocity between the craft and the subsatellite, interferometric ranging is to be used. The precision will be ±1 mgal ($\sim$±3 m), with a resolution on the order of 50-100 km at the earth's surface. The measuring instrument will be a Michelson interferometer, whose laser generator and returning signal detector will be on board the space ship, while the target, i.e. the movable end of the interferometer, is to be a subsatellite equipped with metal reflectors. Variations in radial velocity will result in the oscillation of interference rings in the received signal. It is planned to measure up to 10^5 rings per second. This, together with the parameters of the relative orientations of the laboratory and the subsatellite and the time, are to be stored in computer memory aboard Spacelab.

2.8 Gravitational Gradientometry and the SKYHOOK Project

To understand the idea of an additional project with a subsatellite attached to a space vehicle on an extremely long tether, we first explain the notion of gravitational gradientometry [4, 10, 12].

The gravitational gradientometer is an instrument for measuring the second derivative of gravitational potential along the satellite orbit. It derives from the Eotvos variometer for measuring gravitational gradients. We shall describe the Hughes rotational gravitational gradientometer, which today is perhaps the most promising of several trial designs for a satellite experiment [4, 10, 12]. Imagine two pairs of spheres connected by two rods ar right angles, like a cross, and two such crosses (lying in parallel planes) connected by a hollow rod with at least one spring inside it. The planes of the crosses are perpendicular to the connecting rod, and the axis of the rod is the axis of rotation of the entire satellite which is thus stabilized. In addition, we arrange the axis of rotation very precisely in such a way that it is perpendicular to the plane of the satellite's orbit (Fig. 8 [not reproduced]). The differential torque resulting from varying gradients of the gravitational field affects the individual crosses, giving them different rotations. The twisting of the spring in the connecting tube is measured. The vertical gradient is a combination of three components of the second derivative of the potential, depending on the rotation of the satellite, and these can be determined in this manner.

Laboratory experiments during 1967-1969 are described in detail in reference 12, together with an analysis of measurements errors. For geodetic uses, a satellite gravitational gradientometer placed in an extremely low orbit could measure small anomalies in the gravitational field with considerable resolution. If we wish to study the details of the gravitational field, we must get as close to the earth as possible. But here the atmosphere has a marked effect. "Drag-free" systems are effective only down to 200 km. The possibility of conducting a large number of orbital corrections is limited by the quantity of fuel which can be carried by the satellite and the time during which the compensation system can function perfectly. Very low altitudes,

APPROVED FOR RELEASE: 2007/02/09: CIA-RDP82-00850R000100050024-9

APPROVED FOR RELEASE: 2007/02/09: CIA-RDP82-00850R000100050024-9

about 100 km above the earth's surface, can be attained by satellites only for extremely short periods; they eventually fall into the atmosphere. Measurements by gravitational gradientometer could produce considerable progress if it could be placed in a subsatellite lowered on a long tether from a space craft. It would be possible to detect certain of the harmonic coefficients of equation (1) with degrees and orders up to $n = m = 90\text{-}150$ [8]. Long-term experiments at such low altitudes (which are too high for balloons and sondes) could deal with atmospheric physics and other subjects. Accordingly the SKYHOOK long-tether satellite has been proposed [8]. It will be implemented from on board the Space Shuttle orbiter.

A wire 100 km (!) long with a sonde--the subsatellite--carrying the gradientometer attached to the end will be lowered from the orbiter at an altitude of about 220 km. According to reference 8 there are several almost equivalent positions for the spacecraft-satellite configuration, in one of which the subsatellite is "under" the space craft with a deviation of 5-15° from the vertical. The authors of the project demonstrate that in principle there is no problem in lowering and raising the wire holding the subsatellite, and that the wire will not tangle, break or heat up. The idea of the subsatellite has been taken up and has new modifications [9].

2.9 Applications of Radiointerferometry in Dynamic Geodesy

Very long base interferometry (henceforth VLBI) is used in astrophysics to determine the precise positions of radio emitters and has made possible the introduction into astronomy (radioastrometry) of absolute measurements of the positions of stars (±0.0005" in the determination of directions with repeated measurements, which is an order of magnitude improvement over the best current star catalogs) and has promise in geodesy, geodynamics and celestial mechanics owing to its great accuracy.

The principle of VLBI is simple (the technology is complex and expensive). At at least two separate locations, radiotelescopes simultaneously receive signals from a radio emitter in space. The time is determined by atomic clocks at each station (to 10^{-14} seconds). From the measured time difference of reception of a wavefront of the same signal and the speed of propagation of light, the distance between the radiotelescopes can be calculated [45, 53]. Current technology makes it possible to measure a time difference to ±0.1 nanosecond, and accordingly to measure the distance between the radiotelescopes to within ±10 cm (which is at least equal to the accuracy of determination of the distance between observation stations by laser methods). Variations in the speed of the earth's rotation and variations in the earth's poles can be measured to within ±0.2 msec and ±5 cm respectively.

3. Conclusion

We have examined various methods by which satellites (excluding 2.9) may be used to refine our knowledge of the gravitational field. Some are already standard, while others are in the experimental stage or still being planned. We have observed a great variety of approach to the solution, and sometimes

APPROVED FOR RELEASE: 2007/02/09: CIA-RDP82-00850R000100050024-9

APPROVED FOR RELEASE: 2007/02/09: CIA-RDP82-00850R000100050024-9

extremely unusual methods. All modern methods (except 2.4) require complex and costly equipment. The reader may be interested in the status of our own research into this area.

At present, we generally observe satellites optically, with photographic cameras and laser ranging systems. We are taking part in international observation projects. Doppler measurements are also in preparation. The INTERKOSMOS 17 satellite carries metal reflectors produced in Czechoslovakia; it is currently being tracked, and we intend to work on the analysis of its orbit. But even with the previous INTERKOSMOS satellites, whose orbital parameters were supplied by the Institute of Space Research in Moscow, we were able to determine the parameters characterizing the speed of rotation of the upper atmosphere, its density and the linear combination of harmonic coefficients for orbital resonance (see above). We have taken part in the processing of microaccelerometer data from the French D-5-B satellite (see 2.53).

Our work to advance most of the modern methods discussed here, however, can for the present be only theoretical in character.

Acknowledgements

Warm thanks to Dr of Sciences L. Sehnal, chairman of COSPAR Working Group No 1, for the loan of relevant specialized materials.

BIBLIOGRAPHY

1. R. R. Allan. PLANET. SPACE. SCI. 21, 1973, pp 205-225.

2. R. J. Anderle. "Ocean Geodesy Based on Geos-3 Satellite Altimetry Data," COSPAR, Tel Aviv, Israel, 1977.

3. "Apollo-Soyuz Geodynamics Experiment," COSPAR, Philadelphia, 1976 (from preliminary materials of Working Group No 1).

4. G. Balmino. "La Geodynamique Spatiale" [Space Geodynamics], Flight School, Lannion, CNES, France, 1974, pp 274-471.

5. G. Balmino; C. Reigber; and B. Moynot. "A Geopotential Model Determined From Recent Satellite Observing Campaigns," GRIM 1, IAG/IUGG, Grenoble, 1975.

6. G. Balmino; C. Reigber; and B. Moynot. DEUTSCHE. GEODAT. KOMM. BAYER. AKAD. WISS., A, Heft 86, Munich, 1976.

7. D. C. Brown. "The Use of Artificial Satellites for Geodesy and Geodynamics" (symposium, Athens 1973), 1974, pp 135-155.

8. G. Colombo; E. M. Gaposchkin; M. D. Grossi; and G. C. Weiffenbach. "Long-Tethered Satellites for the Shuttle Orbiter," Center for Astrophysics Preprint Series No 314, presented at international conference on "Technology of Sci. Space Experiments," Paris, 1975.

APPROVED FOR RELEASE: 2007/02/09: CIA-RDP82-00850R000100050024-9

APPROVED FOR RELEASE: 2007/02/09: CIA-RDP82-00850R000100050024-9

9. G. Colombo; D. A. Arnold; H. J. Binsack; R. H. Gay; M. D. Grossi; D. A. Lautmann; and O. Orringer. SMITHS. ASTROPHYS. OBS. REP. IN GEOASTRONOMY, No 2, 1976.

10. W. R. Cordova. "New Concepts in Geodetic Instruments," in "The Changing World of Geodetic Science," Rep. OSU, No 250, Vol. 1, 1977, pp 73-97.

11. D. H. Eckhardt; and G. Hadgigeorge. "Geos-3 Altimetry Reductions in the Australia-New Zealand Region," COSPAR, Israel, 1977.

12. R. L. Forward. Symposium, "The Use of Artificial Satellites for Geodesy and Geodynamics (Athens, 1973), 1974, pp 157-192.

13. V. Dimitrijevich. "Harmograv, D.M.A.A.C." (TP 75-003, 1975, presented at IAG/IUGG Meeting), Grenoble, 1975.

14. E. M. Gaposchkin. SAO SPEC. REP. 353, 1973.

15. E. M. Gaposchkin. Preprint Series No. 324, Center for Astrophysics, Cambridge (report at COSPAR conference, Varna, 1975).

16. E. M. Gaposchkin. SPACE RESEARCH XVII, 1977, pp 63-71.

17. E. M. Gaposchkin; and K. Lambeck. SAO SPEC. REP. 315, 1970.

18. H. Hiller; and D. G. King-Hele. PLANET. SPACE SCI. 23, 1975, pp 511-520.

19. D. G. King-Hele; D. M. C. Walker; and R. H. Gooding. PLANET. SPACE SCI. 23, 1975, pp 229-246.

20. D. G. King-Hele; D. M. C. Walker; and R. H. Gooding. PLANET. SPACE SCI. 23, 1975, pp 1239-1256.

21. J. Klokocnik. BULL. ASTRONOM. INST. CZECH., 28, 1977 pp 293-300.

22. J. Klokocnik. BULL. ASTRONOM. INST. CZECH., 27, 1976, pp 287-295.

23. J. Klokocnik. GAKO, 5, 1976, pp 121-127.

24. J. Klokocnik. BULL. ASTRONOM. INST. CZECH., 28, 1977, pp 291-299.

25. J. Klokocnik; and J. Kostelecky. BULL. ASTRONOM. INST. CZECH., 29, 1978, pp 9-13.

26. K. R. Koch. NOAA/NOS Techn. Rep. 62, Rockville, 1974.

27. Hopkins Univ. Group. "A Satellite Freed of All But Gravitational Forces: TRIAD 1," in "The Uses of Artificial Satellites for Geodesy and Geodynamics" (symposium, Athens 1973), 1974, pp 135-155.

APPROVED FOR RELEASE: 2007/02/09: CIA-RDP82-00850R000100050024-9

APPROVED FOR RELEASE: 2007/02/09: CIA-RDP82-00850R000100050024-9

28. M. Kumar; and I. I. Mueller. "Detection of Crustal Motion Using Spaceborne Laser Ranging Systems," presented at International Symposium on Satellite Geodesy, Budapest, 1977.

29. M. Grun et al. "Review of Cosmonautics," Chapter 2 of P. Lala, "Astrodynamika," National Pedagogic Institute and Stefan Observatory, Prague, 1970.

30. P. Lala et al. "The Results of the Determination of Non-Gravitational Forces From the D-5-B Microaccelerometer," COSPAR, Israel, 1977.

31. B. Lange. "The Drag-Free Satellite," AIAA JOURNAL, 2, 9, 1964, pp 1590-1606.

32. C. D. Leitao; and J. T. McGoogan. ACTA ASTRONAUT. 3, 1976, pp 459-469.

33. F. J. Lerch; J. A. Richardson; and J. E. Brownd. NASA GSFC Doc. X-921-74-145, 1974.

34. C. A. Lundquist. SAO SPEC. REP. 248, 1967.

35. C. A. Lundquist; and G. Veis. SAO SPEC. REP. 200, Vol. 1, 1966.

36. C. A. Lundquist; G. E. O. Giacaglia; K. Hebb; and S. G. Mair. SAO SPEC. REP. 294, 1969.

37. J. G. Marsh; and E. S. Chang. SPACE RESEARCH XVII, 1977, pp 43-48.

38. R. S. Mather; R. Coleman; C. Rizos; and B. Hirsch. "A Preliminary Analysis of Geos-3 Altim. Data in the Tasman and Coral Seas," presented at International Symposium on Satellite Geodesy, Budapest 1977.

39. R. H. Rapp. Ohio St. Univ. Rep. Dept. Geodet. Sci. No. 251, 1977.

40. C. Reigber. DEUTSCHE GEODAT. KOMM. BAYER. AKAD. WISS., C, Heft 198, Munich, 1974.

41. C. Reigber; and G. Balmino. "14th-Order Harmonics From Analysis of Mean Longitude Variations of Resonant Satellites," COSPAR, Philadelphia, 1976.

42. "Report of COSPAR WG-1 for 1975-1976," COSPAR, Philadelphia, 1976.

43. P. Rouchel; L. Castel; and G. Balmino. "Results of a Low-Low Satellite-to Satellite Tracking Simulation Study Between Spacelab and a Sub-Satellite," IAF XXVIII Congress, Prague 1977.

44. L. Sehnal; and J. Kolkocnik. BULL. ASTRONOM. INST. CZECH., 30, 1979, in press.

APPROVED FOR RELEASE: 2007/02/09: CIA-RDP82-00850R000100050024-9

APPROVED FOR RELEASE: 2007/02/09: CIA-RDP82-00850R000100050024-9

45. V. S. Troitskiy. "Radiointerferometry in Astronomy and Geodesy," ZEMLYA I VSESELENNAYA, No 4, 1976 [in Russian].

46. R. A. Van Patten; and C. W. F. Everit. CELESTIAL MECHANICS 13, 1976, pp 429-447.

47. S. Vincent; and J. G. Marsh. "The Use of Artificial Satellites for Geodesy and Geodynamics" (symposium, Athens 1973), 1974, pp 825-855 (especially 849, from which map was taken).

48. C. A. Wagner. NASA GSFC Doc. X-921-76-187, 1976.

49. C. A. Wagner; and S. M. Klosko. NASA GSFC Doc. X-921-75-187, 1975.

50. C. A. Wagner; and F. J. Lerch. J.G.R. 82, 5, 1977, pp 901-914.

51. D. M. C. Walker. PLANET. SPACE SCI. 25, 1977, pp 337-342.

52. W. T. Wells; K. L. Borman; J. T. McGoogan; and C. D. Leitao. "Generation of an Ocean Geoid Map Using Satellite Altimetry Data," COSPAR, Varna, 1975, SPACE RESEARCH XVI, 1976, pp 65-72.

53. I. D. Zhongolovich. "Possibilities for Determining Geodesic and Astrometric Parameters Using Very Long Base Radiointerferometry," [in Russian], presented at International Seminar on Satellite Geodesy, Budapest 1977.

Received 13 February 1978.

Read by Engineer Josef Kabelac, SvF [branch], Czech Institute of Technology, Prague

[Captions] Fig. 1. Satellite S, geocenter (center of mass of the earth) G, topocenter (ground observation station) T, geocentric satellite vector r and station vector R, topocentric satellite vector .

Fig. 2. Parameters of a Satellite Orbit.

Fig. 3. Illustrative Geometric Interpretation of Harmonic Coefficients.

Fig. 4. Shape of Detailed Gravimetric Geoid Based on a Combination of the GSFC GEM 6 Model of the Earth and 1 x 1° Gravitational Anomalies.

Fig. 5. Principle of Satellite Altimetry.

Fig. 6. Comparison of the Shape of the Altimetric Geoid With the Geoid From the Gem 6 Earth Model.

Fig. 7. Principle of Satellite-to-Satellite Tracking.

APPROVED FOR RELEASE: 2007/02/09: CIA-RDP82-00850R000100050024-9

APPROVED FOR RELEASE: 2007/02/09: CIA-RDP82-00850R000100050024-9

Fig. 8. Principle of the Gravitational Gradientometer for Satellite Measurement.

COPYRIGHT: SNTL--Nakladatelstvi Technicke Literatury, 1978.

9427
CSO: 8112/1058

APPROVED FOR RELEASE: 2007/02/09: CIA-RDP82-00850R000100050024-9

APPROVED FOR RELEASE: 2007/02/09: CIA-RDP82-00850R000100050024-9

CZECHOSLOVAKIA

621.181.6
621.311:621.039

STEAM GENERATOR CALCULATIONS FOR BOHUNICE V-1 REACTOR

Prague JADERNA ENERGIE in Slovak No 1, 1979 pp 2-7

[Article by Josef Zadrazil and Vincent Polak, Institute of Nuclear Power Stations, Jaslovske Bohunice: "Computation of Steam Generator Operating Characteristics for the V-1 Power Station in Steady-State Operation"]

[Text] This article presents a theoretical computational model for determining steady-state operating characteristics of the steam generators of the V-1 nuclear power station. A computation procedure was developed on the basis of commonly-used formulas and the nature of the heat-exchange surfaces, and calculations were made for proposed operating conditions. The computation results are discussed in terms of selection of the magnitudes of critical factors, and the effects of these factors on operating characteristics are examined. Computation results are derived for the design parameters and ways of refining the model on the basis of measurements are indicated.

1. Introduction

At the start of power generation and in the course of long-term operation of a nuclear power station, there frequently arises the problem of understanding or forecasting the behavior of the main units and circuits of the power station under unchanging operating regimes or production conditions which are not covered in the computational documents and guarantees from the manufacturers of the equipment. Another problem is that of knowing the operating parameters in some detail, especially in active locations and those parts of the equipment where measurements cannot be taken. For these reasons, the Institute of Nuclear Power Stations in Jaslovske Bohunice has begun developing mathematical models of operating regimes, as well as computational programs which can be used for rapid evaluation of the state and behavior of the equipment operating in the V-1 power station. One of the main units in the power station, whose characteristics must be monitored and evaluated during operation, is the steam generator. The purpose of this article is to compute the thermophysical characteristics of this equipment during steady-state operation.

APPROVED FOR RELEASE: 2007/02/09: CIA-RDP82-00850R000100050024-9

APPROVED FOR RELEASE: 2007/02/09: CIA-RDP82-00850R000100050024-9

2. Main Computational Formulas

The steam generator of the V-1 station, with the designation PGV-4E [1,2], is of the horizontal type. Inside the unit are the heat-exchange surfaces, in the form of U-shaped tubes lying in the horizontal plane; the pipes end in the walls of collectors connected to the primary loop. The steam generator unit contains a separator and a water feed system.

The main function of the steam generator, that of transfe: ..ng heat energy and producing saturated steam, can be described by the equations given below.

For the heat flux passing out of the primary coolant, the following equation applies:

$$Q_1 = m_1 . \Delta i, \qquad (1)$$

where m_1 is the mass coolant flow and Δi is the difference between the input and output enthalpies of the coolant for the section of the exchange surfaces under consideration.

The heat flux may also be determined from the formula for heat transfer through the exchange surface:

$$Q_2 = \frac{\Delta t . S}{\frac{1}{\alpha_1} \cdot \frac{d_1}{d_1} + \frac{d_2}{2.\lambda_M} . \ln \frac{d_2}{d_1} + \frac{1}{\alpha_2}}, \qquad (2)$$

where Δt is the mean arithmetical or logarithmic temperature difference between the coolants on the primary and secondary sides, d_1 and d_2 are the internal and external diameters respectively of the heat-exchange tubes, α_1 and α_2 are the heat transfer coefficients for the inner and outer walls of the tubes respectively, λ_M is the heat conductivity of the pipe material and S is the heat exchange surface with diameter d_2.

To determine the heat transfer coefficients for clean transfer surfaces before they have been used, the equation presented in references [3, 4] was used:

$$\alpha_1' = 0{,}023 \frac{\lambda_1}{d_1} \mathrm{Re}_1^{0.8} . \mathrm{Pr}_1^{0.4}, \qquad (3)$$

where λ_1 is the unit heat conductivity, Re_1 is the Reynolds number and Pr_1 is the Prandtl number for the coolant on the primary side; the formula used for the heat exchange coefficient for a large volume of boiling water on the secondary side is:

$$\alpha_2' = A . q^{0.7}, \qquad (4)$$

where q is the flux density and the parameter A depends on the thermophysical properties of the water-steam mixture at the pressure in the steam generator drum.

During operation of a nuclear power station, free oxygen which is present in the primary coolant as a radiolysis product creates an oxide layer on the heat exchange surface. This layer has a certain thermal resistance, and accordingly

APPROVED FOR RELEASE: 2007/02/09: CIA-RDP82-00850R000100050024-9

APPROVED FOR RELEASE: 2007/02/09: CIA-RDP82-00850R000100050024-9

it is suggested that the heat transfer coefficient for a stainless steel surface during operation be decreased by a correction factor $k_1 = 0.90\text{-}0.95$ [3] according to the equation $\alpha_1 = k_1 \cdot \alpha_i'$.

Similarly, during operation the feedwater in the secondary circuit taken on impurities such as chlorine and the like, which create oxide layers on the tube surface, so that at relatively high heat flux densities the coefficient α_2 is decreased. This decrease can be expressed by the equation

$$\alpha_2 = \frac{1}{\frac{1}{\alpha_2'} + k_2}, \qquad (5)$$

where the value $8.59845 \cdot 10^{-3}$ m^2-deg/kW ($1.0 \cdot 10^{-5}$ m^2-deg-hr/kcal) [3] or a larger value [4] is suggested for the thermal resistance k_2 of the oxidized layer on the steel surface.

We may set up a balance equation (ignoring heat losses) for the heat flux from the steam generator to the process equipment in the secondary loop:

$$Q_2 = m_p(i_p - i_{NV}) + m_0(i_0 - i_{NV}), \qquad (6)$$

where m_p is the steam output, m_0 is the blowdown or drain [odluh, odkal] mass flow, i_p is the enthalpy of the wet steam produced (with dryness s), i_0 is the enthalpy of the blowdown or drainage water, and i_{NV} is the enthalpy of the feedwater.

The steam produced in the water volume of the steam generator passes through the evaporation surface and drops of water separate from in the the steam volume of the drum. To calculate the humidity of the steam after this separation we may use Sterman's formula [3]:

$$\omega = 0{,}211 \frac{w_p^{2,76}}{h_p^{3,5}} M \quad [\%], \qquad (7)$$

where w_p (m/sec) is the speed of the steam passing from the evaporating surface, h_p (m) is the height of the steam column above the evaporation surface (when the column is higher than 0.8 meters, $h_p = 0.8$ must be used in the equation), and M is a parameter dependent on the thermophysical properties of the steam-water mixture on the boundary curve under the pressure in the drum; at the rated pressure of 4.61 MPa it is equal to 13.67.

3. Computation Procedure

The steam generator of the V-1 station has replaceable tubes so located in the drum that they fill the water space as completely as possible. Accordingly the individual tubes range from 7 to 11.5 meters in length. This results in a considerable variation in heat transfer and steam production in individual sectors of the steam generator, and accordingly during calculation it is advantageous to take account of this circumstance.

For calculation, the bundle of tubes was divided into two parts according to length, and also into two parts according to position in relation to the

APPROVED FOR RELEASE: 2007/02/09: CIA-RDP82-00850R000100050024-9

APPROVED FOR RELEASE: 2007/02/09: CIA-RDP82-00850R000100050024-9

collector. An average tube length was determined for each sector, and these average lengths were used to calculate the operating parameters for the sectors.

The average tube lengths were used to determine the mass flow distribution for the primary coolant from its calculated speed.

For this purpose we made the assumption that for tubes with different lengths and otherwise identical geometry and identical overall pressure drops, only the friction loss coefficients differed. Since for the primary coolant flow rates generally occurring in a steam generator during power production the friction loss coefficient is independent of the Reynolds number, the mass flow ratio for two tubes can be determined by the equation

$$\frac{m_1}{m_2} = \sqrt{\frac{l_2}{l_1} \cdot \frac{\bar{\varrho}_1}{\bar{\varrho}_2}}, \qquad (8)$$

where l_i are the tube lengths and $\bar{\varrho}_i$ are the average specific gravities of the coolants; within the operating parameter range it was determined that the ratio of these two specific gravities can be taken as 1. Equation 8 is valid if we neglect the dependence of output and input losses on flow rate variations within the range in question. In view of the relatively large variation in the temperature difference Δt along the tubes, for computation purposes we must divide the whole tube lengths into several sections (parts) so that in each part the condition

$$t_K - t_S > t_A - t_E, \qquad (9)$$

for use of the exchange-surface heat transfer equation is met; here t_A is the input and t_E the output temperature of the primary coolant for the section in question, and t_S is the saturation temperature of the water under the pressure in the drum.

An additional decisive factor in choosing the length of the first section was the length of the feedwater tube which would make it possible to determine the water quantity between the tube bundles in which the feedwater would be heated to the saturation temperature. The length of the third section was chosen with reference to the geometry of the bundles.

The division of the transfer surfaces into sectors for computation is shown schematically in Fig. 1.

In view of the variable speed of the coolant in the tubes on the primary side, we found the Reynolds number for that side in the most suitable form for determining heat transfer:

$$\mathrm{Re} = \frac{4 \cdot m}{\pi \cdot d_1 \cdot \eta}, \qquad (10)$$

where m is the coolant mass flow in the tube in question, and the dynamic viscosity η depends only on coolant temperature or sometimes pressure.

APPROVED FOR RELEASE: 2007/02/09: CIA-RDP82-00850R000100050024-9

APPROVED FOR RELEASE: 2007/02/09: CIA-RDP82-00850R000100050024-9

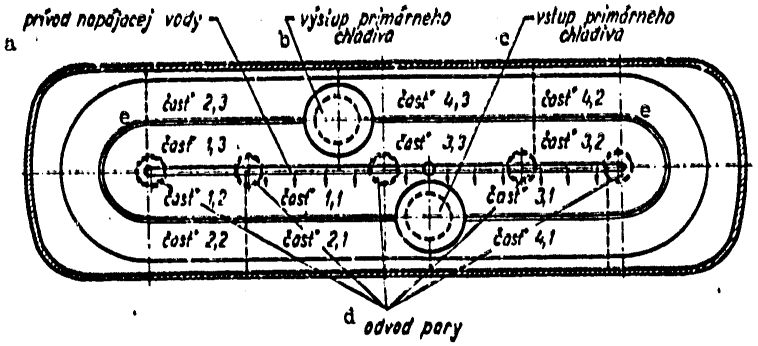

Fig. 1. Schematic Horizontal Section of V-1 Power Station Steam Generator.

Key: a. Feedwater
b. Primary coolant inlet
c. Primary coolant outlet
d. Steam outlet
e. Sectors 1.1, 1,2...

In view of the lack of reliable and practically-oriented references on the variation of hydraulic resistance along the primary coolant path in the steam generator, we calculated pressure losses on the basis of a nominal value obtained as the ratio of the squares of the respective mass flows and coolant densities; because of the small pressure losses, in calculating the thermophysical properties of the coolant we used the average steam generator pressure throughout.

The transfer of thermal energy from the primary coolant can be calculated in simple fashion by solving the equation $Q_1 = Q_p$, which entails solving the expressions in formulas (1) and (2). This equation was solved for the temperature for the primary coolant on exiting from each calculation sector by a computer iteration method with provision for specifying the level of precision; the calculation proceeded sector by sector along the length of the tubes in each bundle. In view of the relatively small temperature difference, the average temperature of a given sector was used in calculating the thermophysical properties of the coolant and transfer surface material in the transfer equations. The temperature of the primary coolant at the outlet collector of the steam generator was determined from the temperatures on exiting from the individual bundles of tubes. From the computation formulas used it is clear that at a constant operating pressure in the drum, the other operating parameters of the secondary circuit do not influence the heat transfer value, so that it may be used in determining the characteristics of the primary and secondary circuits during computation of the characteristics of the power station block as a whole [6, 7].

APPROVED FOR RELEASE: 2007/02/09: CIA-RDP82-00850R000100050024-9

APPROVED FOR RELEASE: 2007/02/09: CIA-RDP82-00850R000100050024-9

In the preceding paragraph we described the course of calculation of the thermal fluxes Q_p given up to the coolant in the secondary circuit in the individual sectors. These fluxes produce in sections 1.1 and 3.1 heating of the feedwater to the saturation temperature corresponding to the pressure in the drum, and in all sections steam is produced; the quantity is governed by the dryness calculated after its separation in the steam volume, by the amount of blowdown or drainage (which for simplicity was assumed to be in proportion to the amount of steam produced), and finally by the magnitude of the heat losses around the generator shell (accounted for in the calculation by the thermal efficiency coefficient η_{pg} of the generator). The equation $Q_p \cdot \eta_{pg} = Q_2$ was set up for each section according to this procedure; equation (6) was suitably adjusted and the present equation solved by iteration on the computer. The resulting steam parameters for the secondary circuit were determined by summing and balancing the heat in all computation sections.

By using this method, the values of the determining factors can be selected and the trends of the thermophysical operating characteristics within the steam generator calculated for individual sections; the operating parameters of the working substances are also calculated at the exits from the primary and secondary circuits. The determining factors in the development and use of this method fall into three groups:

a. adjustable values of operating parameters which are associated with production regimes of the primary and secondary circuits and which include temperature, pressure and mass flow of the primary coolant at the steam generator inlet, and the enthalpy and temperature of the secondary-circuit feedwater;

b. the steam generator parameters themselves, which must be based on measured values in simulation calculations; they include the thermal efficiency of the steam generator, a correction factor for the presence of oxidized (dirty) transfer surfaces, the water level in the steam generator drum, the mass flow in blowdown or drainage, and the pressure in the drum;

c. computational and geometric constants which depend on the calculation procedure and the design of the steam generator.

4. Computation Results and Discussion

Our method was used to develop the SCHPGV1 computer program in FORTRAN IV; computation was carried out on a Tesla 270 computer.

The trends of the thermophysical parameters inside the drum were calculated for 12 distinct calculation sectors. The number of such areas could be increased using our method so as to obtain a better calculation of heat transfer over the full length of the tubes, but this would weaken our assumption that there is no heat transfer or flux in the horizontal direction between individual sections, and would also require a more detailed treatment of the local changes in each sector resulting from blowdown or drainage, introduction of feedwater and removal of steam, as well as from local heat losses.

APPROVED FOR RELEASE: 2007/02/09: CIA-RDP82-00850R000100050024-9

APPROVED FOR RELEASE: 2007/02/09: CIA-RDP82-00850R000100050024-9

In the computation, the geometric constants and basic design parameters were taken from references [1, 2] and the magnitudes of the critical factors were chosen within the range of recommended values following an analysis of computational results by the method described below.

For a number of reasons, the computed thermal efficiency η_{pg} varied between 0.978 and 0.989; but it is clear that the precision with which this value is chosen affects only the computed quantity of steam produced. To make the computations more precise, it will be necessary to make use of measured values for heat loss in the steam generator during operation, while for individual computation sectors it will be necessary to treat heat losses in terms of the corresponding drum surface elements.

To calculate the basic operating characteristics, we analyzed the effect of selection of thermal resistance correction coefficients on the result. This analysis enables us to state that selection of the coefficient k_1 has no fundamental effect on the results within the range of recommended values. The accuracy of determination of thermal resistance k_2 (5), as is shown in Fig. 2, has a considerable effect on the temperature of the primary coolant t_{1E} at the outlet and on steam production m_p. Thus for the planned operating parameters we found $k_2 = (2.0 - 2.5) \cdot 8.59845 \cdot 10^{-3}$ m^2-deg C/kW. We may recommend that the resistance k_2 be specified for a given value of t_{1E} and the heat transfer equations be corrected for the specific situation. Since in practice the value of k_2 depends on the heat conductivity and thickness of the deposited layer, if we know the age of the layer we can determine the degree of "aging" of the transfer surface and thus determine its effect on the steam generator parameters in the interval between cleanings. A more profound analysis of heat transfer would require correction of the equations used for the specific layout and geometry of the transfer surfaces within the boiling water and an understanding of the effect of a nonuniform heat loading of the transfer surfaces on creation of a heat-resistant layer in the individual sectors.

Another important quantity in calculating the operating characteristics is the accuracy of determination of generator drum pressure. The dependence of the main operating characteristics on this pressure (p_B) is shown in Fig. 3 for the design parameters. Even though a pressure $p_B = 4.609$ MPa is prescribed for every production regime, it is clear that within the tolerances set by the regulating organs, process changes lead to variations in this pressure and to corresponding changes in the operating characteristics.

Given the complexity of the steam separation process and the lack of suitable formulas for this type of steam generator, we developed an approximate method for calculating steam separation in the steam space only, neglecting the tendency to separation in the louvered separators mounted in the upper part of the drum, which would be most pronounced primarily at high humidities [5]. The calculations were made for various changes in the main operating parameters and particularly for changes in the water level h_y above the upper row of exchange tubes. The final steam dryness resulting from mixture of steam from various sectors in the outlet collector is shown in Fig. 4 as a function of the height h_y for the design parameters; separation in the entire steam space was taken into account. Following analysis of the computation and

APPROVED FOR RELEASE: 2007/02/09: CIA-RDP82-00850R000100050024-9

APPROVED FOR RELEASE: 2007/02/09: CIA-RDP82-00850R000100050024-9

comparison of the results with measured values obtained in the USSR for a similar steam generator, we may recommend that separation in the steam space under the louvered separator be used for approximate computation of steam dryness. The calculated dryness is slightly high and its trend after the characteristic break point more favorable than that of the measured values; this is caused by a change in the steam volume as the surface rises owing to an uneven steam load, by poorer steam separation in the vicinity of the outlets from the drum and by other design factors.

Another factor which particularly affects calculation of the heat balance on the secondary side and thus also the accuracy of determination of steam production, is the quantity and composition of the blowdown or drainage from the steam generator in various regimes. To make the computations accurate, it is helpful to use local effects of blowdown or drainage withdrawal and to include them in computations for individual sectors.

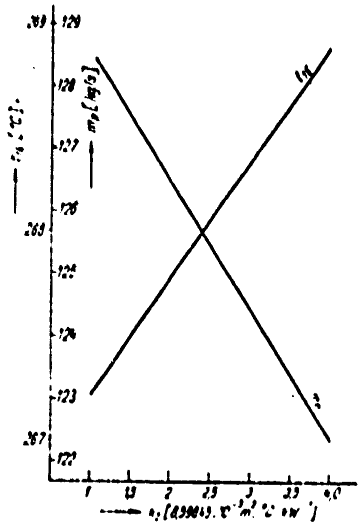

Fig. 2. Dependence of Steam Generator Characteristics on Thermal Resistance (k_{ℓ}).

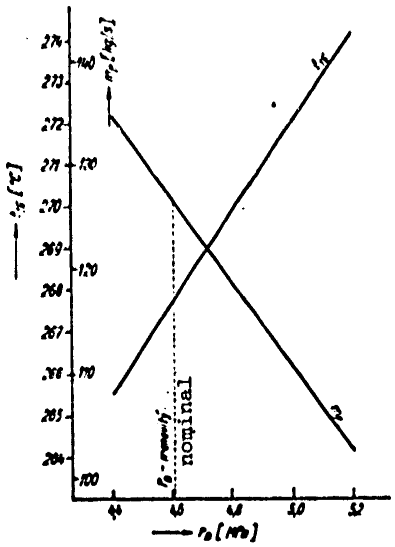

Fig. 3. Dependence of Steam Generator Characteristics on Pressure Inside the Drum.

In most calculations made for the assumed range of critical operating characteristics, we used as the planned operating parameters computed values of the main thermophysical quantities in the individual sectors of the steam generator, as shown in Table 1. For these characteristic values we can easily see differences among the various sectors; these differences, as stated in the discussion of

APPROVED FOR RELEASE: 2007/02/09: CIA-RDP82-00850R000100050024-9

APPROVED FOR RELEASE: 2007/02/09: CIA-RDP82-00850R000100050024-9

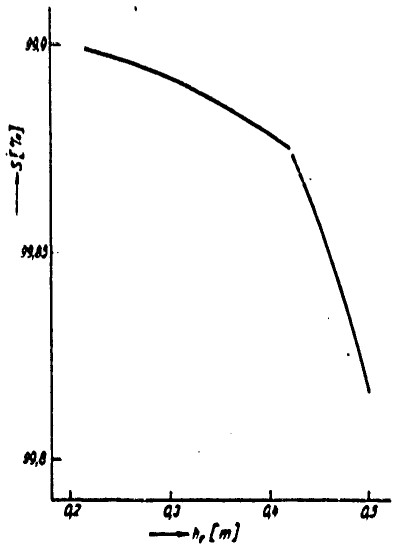

Fig. 4. Dependence of Steam Dryness After Separation in Steam Drum on Height of Water in Drum.

APPROVED FOR RELEASE: 2007/02/09: CIA-RDP82-00850R000100050024-9

APPROVED FOR RELEASE: 2007/02/09: CIA-RDP82-00850R000100050024-9

results, are likely to be even more pronounced if we take into account local effects in the calculation of heat transfer and withdrawal. These differences also give an impression of the loads on individual parts of the transfer surfaces.

Table 1. Values of Thermophysical Quantities for Individual Sectors of the Steam Generator.

Označenie oblasti 1	Teplota primárneho chladiva na výstupe [°C] 2	Celkový koeficient prestupu tepla [kW.m^{-2}.°C^{-1}] 3	Stredný teplotný rozdiel [°C] 4	Stredná rýchlosť pary na výstupe z výpar. hladiny [m.s^{-1}] 5	Suchosť pary po separácii v parnom objeme [%] 6
1,1	285,0	5,053	33,65	0,277	99,86
1,2	274,7	4,682	21,03	0,265	99,88
1,3	269,2	4,186	13,11	0,134	99,98
2,1	284,0	4,867	33,13	0,282	99,85
2,2	269,1	4,302	16,56	0,113	99,98
2,3	265,7	3,497	8,49	0,052	99,99
3,1	285,5	5,057	33,87	0,278	99,86
3,2	274,7	4,691	21,24	0,268	99,87
3,3	269,2	4,184	13,10	0,134	99,98
4,1	284,5	4,871	33,36	0,283	99,85
4,2	269,1	4,313	16,74	0,114	99,98
4,3	265,7	3,499	8,50	0,052	99,99

Key:
1. Sector
2. Input temperature of primary coolant
3. Overall heat transfer coefficient
4. Average temperature difference
5. Average speed of steam leaving evaporation surface (m/sec)
6. Dryness of steam after separation in steam space

The characteristic curve of the steam generator as a whole on the primary side is shown graphically in Fig. 5. It can be seen that the output temperature is rather stable, as a result of the nature of saturated steam production, but in view of the rather small overall temperature drop (maximum about 31° C) and the large heat flux, the computation formulas used demand accurate determination of the output temperature; demands on control measurement during operation are also high.

Fig. 6 shows the dependence of the amount of steam produced in the generator on feedwater temperature t_{NV} and temperature t_{1A} for $m_1 = 1{,}404.86$ kg/sec.

In determining the operating characteristics of the steam generator it is necessary also to take into account the change (decrease) in the transfer surface resulting from clogging of tubes which have been damaged. This decrease results in lower output and in proportional to the number of tubes failing.

APPROVED FOR RELEASE: 2007/02/09: CIA-RDP82-00850R000100050024-9

APPROVED FOR RELEASE: 2007/02/09: CIA-RDP82-00850R000100050024-9

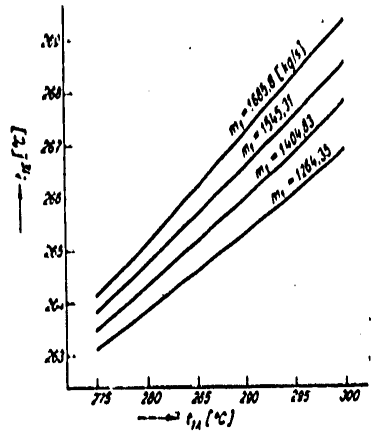

Fig. 5. Steam Generator Characteristic Curve on Primary Side

Key: t_{1A}, t_{1E}: inlet and outlet temperatures of primary coolant.
m_1: mass flow.

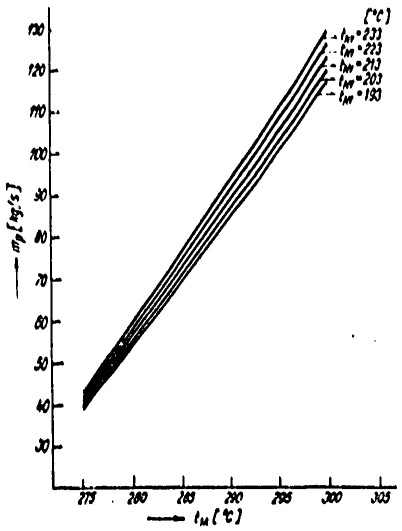

Fig. 6. Steam Production Characteristoc Curves

Key: t_{1A}: primary coolant inlet temperature.
mp: steam production.
t_{NV}: feedwater temperature.

5. Conclusions

The theoretical model for determining operating characteristics of the steam generator and the calculations which have been made enable us before operation of the nuclear power station to obtain an idea of the thermophysical relationships in the steam generator drum, where it is always difficult to conduct running measurements, and also an idea of its external behavior in various production regimes, and thus to determine the relationship between the primary and secondary loops during operation.

Through analysis of the computational formulas and the results we have determined possibilities and directions for further refinement; but it is always necessary to consider whether further refinements can be checked by measurement. The computation results and programs will be used during startup and initial operation of the V1 station and in tracking and evaluating operating parameters and balancing heat production. In research, these results will be used especially to develop technical and economic models of the operation of a nuclear power station and in optimization of its parameters.

APPROVED FOR RELEASE: 2007/02/09: CIA-RDP82-00850R000100050024-9

APPROVED FOR RELEASE: 2007/02/09: CIA-RDP82-00850R000100050024-9

On the basis of measurements conducted in the USSR, more refined equations published in the literature and operating measurements on the V1 power station, we will continue efforts to correct and adjust the theoretical model, particularly as regards heat transfer and steam separation, with the aim of producing a reliable computational model for determining steady-state operating characteristics of steam generators of this type and for investigating possibilities of improving the generators and their operation.

BIBLIOGRAPHY

1. The Bohunice V1 Power Station in the CSSR. Engineering Plans [in Russian]. Leningrad, Teploelektroproyekt, 1972.

2. Documentation accompanying delivery of PGV-4E steam generator from USSR, installation drawing 180-01-001.

3. T. Ch. Margulova. Nuclear Power Station Steam Generator Calculations and Design [in Russian]. Moscow-Leningrad, GEI, 1962, pp 62, 64.

4. S. S. Kutateladze; and V. M. Borisanskij. Heat Transmission Handbook [in Czech]. Prague, SNTL, 1962, p 215.

5. T. Ch. Margulova. Methods of Producing Clean Steam. Moscow-Leningrad, GEI, 1955, p 50.

6. J. Zadrazil et al. EBO [Bohunice Nuclear Power Station] Research Report No 10/75. Jaslovske Bohunice, EBO, 1975, pp 109-113.

7. J. Zadrazil et al. VUJE [Institute of Nuclear Power Stations] Research Report No 11/77. Jaslovske Bohunice, VUJE, 1977, pp 144-146.

Received 28 March 1978.

COPYRIGHT: SNTL - Nakladatelstvi Technicke Literatury n.p., 1979

9427
CSO: 2402

END

APPROVED FOR RELEASE: 2007/02/09: CIA-RDP82-00850R000100050024-9